

Temperature-resolved *in situ* X-ray absorption spectroscopic study on the reduction of nanostructured Fe₂O₃ within the pore system of mesoporous carbon CMK-1

Holger Huwe and Michael Fröba*

Institute of Inorganic and Analytical Chemistry, Justus Liebig University Giessen, Heinrich-Buff-Ring 58, 35392 Giessen, Germany. E-mail: michael.froeba@anorg.chemie.uni-giessen.de

Results of *in situ* X-ray absorption spectroscopy experiments on the reduction of thin-layered nanostructured X-ray amorphous iron(III) oxides inside the pore system of mesoporous carbon CMK-1 are presented. These *in situ* measurements were carried out using 4% hydrogen in nitrogen as reduction gas over a 300–1000 K temperature range. The thermochemical behaviour of the nanostructured materials was compared with that of the bulk phases. The spectra series examined by factor analysis gave a good insight into the reduction products of iron oxide nanoparticles occurring in mesoporous carbon CMK-1.

Keywords: XAFS; *in situ*; nanostructured iron oxide; mesoporous carbon; reduction; host structure.

1. Introduction

The reduction behaviour of 3d metal oxides has been investigated for more than a century, particularly for the system $\text{Fe}_2\text{O}_3 \rightarrow \text{Fe}_3\text{O}_4 \rightarrow \text{Fe}_{1-x}\text{O} \rightarrow \text{Fe}^0$ for which multiple experimental and theoretical studies have been carried out. In fact, the members of this group act in a sense often as model compounds for the varieties of transition metal oxides. This system was chosen owing to its application in *e.g.* catalysis or in potential hydrogen storage. Many experiments have been performed in order to learn more about the properties of the iron oxides or to study their redox behaviour, resulting in numerous papers and books (Bajt *et al.*, 1994; Becker *et al.*, 1995; Cornell & Schwertmann, 2003; Darken & Gurry, 1946; de Masi *et al.*, 2002; Dünwald & Wagner, 1931; Fjellvåg *et al.*, 2003; Fröba *et al.*, 1999; Köhn & Fröba, 2003; Köhn *et al.*, 2003; Rao & Moinpour, 1983).

New access to nanosized particles is provided by their synthesis within confined spaces of defined solid host materials. Generally, these spaces are ordered pores which serve as size-limiting matrices for the nanostructured guest species. Very often these host/guest compounds exhibit different physical and chemical properties in comparison with the respective bulk materials. For example the system $\text{Cd}_{1-x}\text{Mn}_x\text{S@MCM-48}$ silica shows strong size dependencies on the magnetic and optical properties of the guest compound (Brieler *et al.*, 2005; Klar *et al.*, 2004); the systems $\text{Fe}_2\text{O}_3\text{@SBA-15}$ silica and $\text{Fe}_2\text{O}_3\text{@CMK-3}$ carbon exhibit catalytic activities different from that of bulk haematite (Minchev *et al.*, 2005; Tsoncheva *et al.*, 2004). Depending on the reaction conditions it is also possible to form different

nanostructured phases, *e.g.* magnetite owing to the intra-pore reduction of haematite, an example we will examine in this study. For a deeper insight into the redox behaviour of metal oxides, *in situ* X-ray absorption spectroscopy (XAS) is a very good probe for investigating these properties.

The present work undertakes the first study on the reduction behaviour of nanosized iron(III) oxides formed in mesoporous carbon atoms in comparison with the respective bulk materials. Apart from that it shows the potential of *in situ* XAS studies for gaining knowledge (in a simple manner) on redox processes.

2. Synthesis and experimental

Nanostructured X-ray amorphous iron(III) oxides were synthesized inside the pore system of mesoporous carbon CMK-1 (pore diameter ≈ 3 nm), first reported by Huwe & Fröba (2003). The almost exclusive intra-pore formation of these nanosized particles and the preservation of the host structure during the synthesis procedure was proved by powder X-ray diffraction, nitrogen physisorption, transmission electron microscopy, Raman and X-ray absorption spectroscopy.

The *in situ* reductions were carried out in a specially designed and constructed cell (Huwe & Fröba, 2004) at the beamline EXAFS II (E4) at the storage ring Doris III (HASYLAB @ DESY, Hamburg, Germany). All spectra were recorded in fluorescence mode using a single-crystal Ge detector.

For the measurements the nanostructured host/guest compound as well as bulk haematite were pressed into boron

nitride pellets. As reduction gas, 4% hydrogen in nitrogen was used with a flow rate of $25 \text{ cm}^3 \text{ min}^{-1}$. The spectra series were taken in the temperature range 300–1000 K (heating rate 5 K min^{-1}) with a spectrum recorded every 15 K under continuous heating.

The respective series of XANES spectra were analyzed using the program *WinXAS* (Ressler, 1998). After common data reduction procedures a principal component analysis (PCA, factor analysis) (Malinowski & Howery, 1980; Ressler *et al.*, 2000) was carried out with respect to the corresponding reference spectra of the bulk materials. For a discussion of the results one has to take into account that the detection limit of the PCA is about 4–5%. The required reference spectra were recorded from commercially available oxides and metals in nitrogen atmosphere at the temperatures where they occur in the products during the reduction process.

3. Results and discussion

A series of energy-calibrated, normalized and background-corrected spectra of the reduction of Fe_2O_3 @CMK-1 are shown in Fig. 1. Clearly visible is the decrease in the white-line intensity and changes in the EXAFS oscillations during the reduction process. In the XANES a change in the pre-edge region accompanied by an 8 eV shift of the absorption edge to smaller energies for the transformation $\text{Fe}_2\text{O}_3 \rightarrow \text{Fe}^0$ is observed.

The occurrence of the different phases of the host/guest system (extracted from the XANES) is shown in Fig. 2(a). The reduction process starts at about 580 K and ends at about 890 K. The first reduction product is magnetite. The major part of Fe_3O_4 is reached at 683 K (89%). This followed a decrease owing to the formation of Fe_{1-x}O , a non-stoichiometric wüstite phase. At 720 K the partition of Fe_3O_4 is equal to those of Fe_{1-x}O (~48% each). Fe_3O_4 occurs up to ~800 K. The formation of Fe_{1-x}O starts at about 650 K, has a maximum at 760 K (91%) and decreases due to the reduction to Fe^0 .

Fig. 2(b) exhibits the corresponding results for the bulk haematite. At first glance the phases formed are the same, but

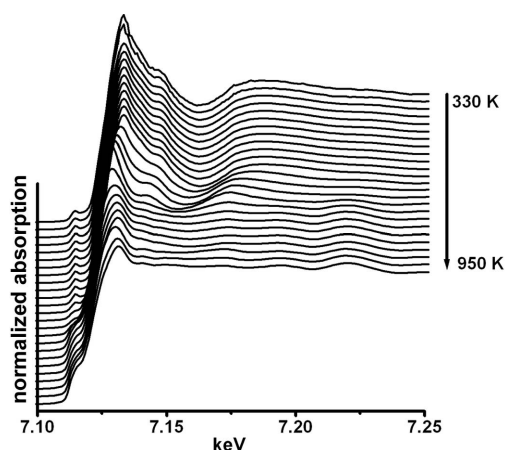


Figure 1
Temperature-dependent *in situ* XAS measurements at the Fe K-edge of Fe_2O_3 @CMK-1 during reduction with hydrogen in nitrogen.

the redox processes take place over a different temperature range. A more detailed presentation is shown in Figs. 3(a) and 3(b). Here the occurrence (as a function of the reduction temperature) of the respective phases in the case of the host/guest compound and the bulk material is compared. The reduction process starts at 650 K for the bulk material and ends at about 800 K. In contrast, the nanostructured host/guest system already begins to react at 580 K, an effect probably caused by the very small particle size (~3 nm) which leads to a higher thermochemical reactivity. In addition, the temperature interval in which the phase transformations occur is two times larger for Fe_2O_3 @CMK-1 ($\Delta T \approx 310 \text{ K}$), an effect which could be due to the intra-pore diffusion limitations for the gaseous species. While for the host/guest compound the reduction to Fe_3O_4 has already reached its maximum (at 683 K), that of bulk haematite has just started. The formation of the bulk Fe_{1-x}O phase has its maximum almost at the same temperature as Fe_{1-x}O @CMK-1, but the reduction to Fe^0 is much faster. Another difference between the host/guest compound and the bulk material is the maximum concentration of the two intermediate phases Fe_3O_4 and Fe_{1-x}O . Owing to the broader temperature range (caused by slower kinetics) the overlap of the different regimes of occurrence is reduced in the case of the host/guest compounds, which results in

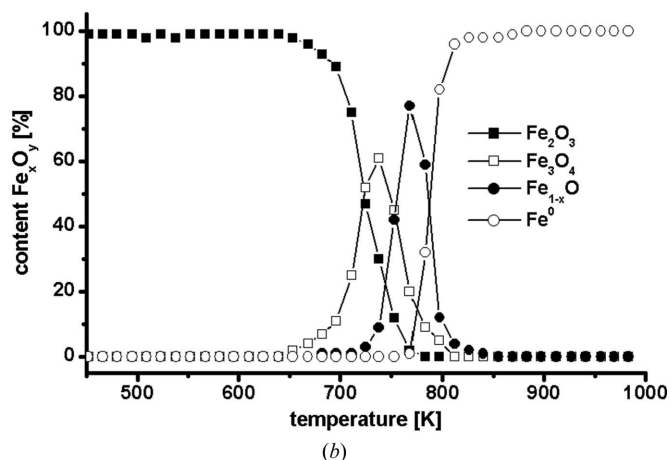
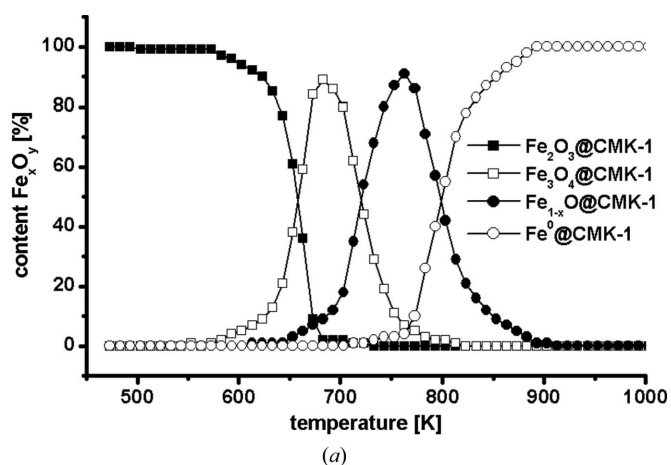


Figure 2
Occurrence of the respective iron oxide phases during the reduction process of (a) Fe_2O_3 @CMK-1 and (b) bulk haematite.

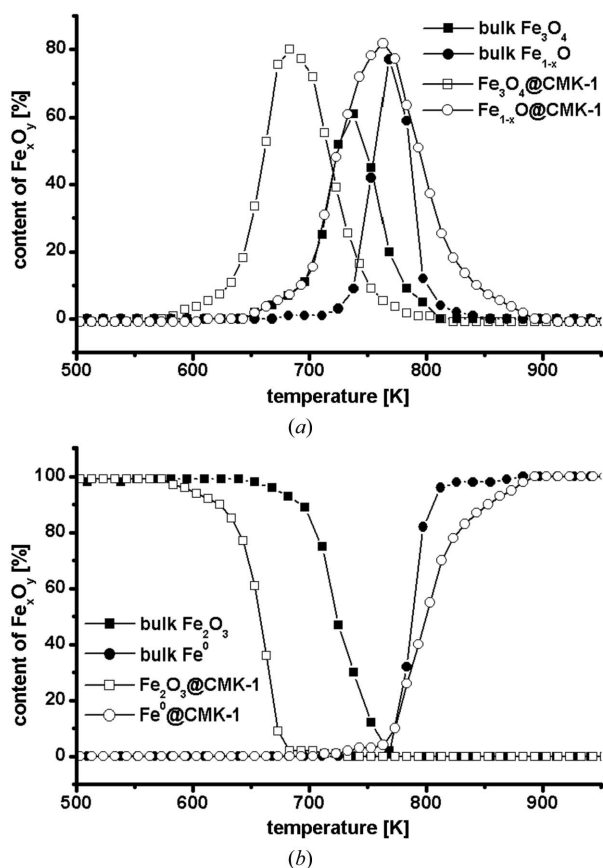


Figure 3 Comparison between the respective iron oxide phases occurring during the reduction process of Fe_2O_3 @CMK-1 and bulk haematite: (a) bulk Fe_3O_4 and bulk Fe_{1-x}O versus Fe_3O_4 @CMK-1 and Fe_{1-x}O @CMK-1; (b) bulk Fe_2O_3 and bulk Fe^0 versus Fe_2O_3 @CMK-1 and Fe^0 @CMK-3.

contents of above 90% for the single phases. In contrast, the bulk material always exhibits mixtures of at least two (sometimes even three) phases which of course decreases the content of the respective majority phase. In general, one can say that the kinetics of the reduction steps $\text{Fe}_2\text{O}_3 \rightarrow \text{Fe}_3\text{O}_4 \rightarrow \text{Fe}_{1-x}\text{O} \rightarrow \text{Fe}^0$ are affected by the spatial and chemical environment. In the case of the host/guest compound the reduction starts at lower temperatures which can be attributed to the much smaller particle size. Nevertheless, there might also be some influence from the carbon host structure which could promote the reduction of the haematite. In conclusion, it seems that in the case of the host/guest system the reduction reactions are not that fast compared with the bulk material, which is probably caused by diffusion limitations. Nevertheless, this allows a much better separation of the respective single phases in comparison with the bulk material, an effect which might be useful for further studies.

4. Conclusion

This study shows the first results on the reduction of iron oxide nanoparticles within a mesoporous carbon CMK-1 host

structure. The thermochemical behaviour was monitored by temperature-dependent *in situ* X-ray absorption spectroscopic measurements. While the reduction of the nanoparticles starts at lower temperatures, the velocity of the following transformations are slowed down in comparison with the bulk material which allows a much better separation of single phases. In summary, one can say that the kinetics of the reduction steps $\text{Fe}_2\text{O}_3 \rightarrow \text{Fe}_3\text{O}_4 \rightarrow \text{Fe}_{1-x}\text{O} \rightarrow \text{Fe}^0$ are mainly affected by the particle size as well as the spatial and chemical environment.

The authors would like to thank HASYLAB@DESY for allocating beam time and financial support. Further financial support by the Justus Liebig University Giessen and the Fonds der Chemischen Industrie is gratefully acknowledged.

References

- Bajt, S., Sutton, S. R. & Delaney, J. S. (1994). *Cosmochim. Acta*, **58**, 5209–5214.
- Becker, K. D., Niemeier, D., Wissmann, S., Oversluizen, M., Couves, J. W. & Chadwick, A. V. (1995). *Nucl. Instrum. Methods*, **B97**, 111–114.
- Brieler, F. J., Grundmann, P., Fröba, M., Chen, L., Klar, P. J., Heimbrodt, W., Krug von Nidda, H.-A., Kurz, Th. & Loidl, A. (2005). *Chem. Mater.* **17**, 795–803.
- Cornell, R. M. & Schwertmann, U. (2003). *The Iron Oxides*. Weinheim: Wiley-VCH.
- Darken, L. S. & Gurry, R. W. (1946). *J. Am. Chem. Soc.* **68**, 798–819.
- Dünwald, H. & Wagner, C. (1931). *Z. Anorg. Allg. Chem.* **199**, 321–319.
- Fjellvåg, H., Hauback, B. C., Vogt, T. & Stølen, S. (2002). *Am. Mineral.* **87**, 347–349.
- Fröba, M., Köhn, R., Bouffaud, G., Richard, O. & van Tendeloo, G. (1999). *Chem. Mater.* **11**, 2858–2865.
- Huwe, H. & Fröba, M. (2003). *Micropor. Mesopor. Mater.* **60**, 151–158.
- Huwe, H. & Fröba, M. (2004). *J. Synchrotron Rad.* **11**, 363–365.
- Klar, P. J., Chen, L., Heimbrodt, W., Brieler, F. J., Fröba, M., Kurz, T., Krug von Nidda, H.-A. & Loidl, A. (2004). *Advances in Solid State Physics*, Vol. 44, edited by B. Kramer, pp. 491–502. Berlin/Heidelberg: Springer-Verlag.
- Köhn, R. & Fröba, M. (2003). *Z. Anorg. Allg. Chem.* **629**, 1673–1682.
- Köhn, R., Paneva, D., Dimitrov, M., Tsoncheva, T., Mitov, I., Minchev, C. & Fröba, M. (2003). *Micropor. Mesopor. Mater.* **63**, 125–137.
- Malinowski, E. R. & Howery, D. G. (1980). *Factor Analysis in Chemistry*. New York: Wiley.
- Masi, R. de, Reinicke, D., Muller, F., Steiner, P. & Hufner, S. (2002). *Surf. Sci.* **516**, L515–L521.
- Minchev, C., Huwe, H., Tsoncheva, T., Paneva, D., Dimitrov, M., Mitov, I. & Fröba, M. (2005). *Micropor. Mesopor. Mater.* **81**, 331–341.
- Rao, Y. K. & Moinpour, M. (1983). *Metall. Trans. B*, **14**, 711–723.
- Ressler, T. (1998). *J. Synchrotron Rad.* **5**, 118–122.
- Ressler, T., Wong, J., Roos, J. & Smith, I. L. (2000). *Environ. Sci. Technol.* **34**, 950.
- Tsoncheva, T., Paneva, D., Mitov, I., Huwe, H., Fröba, M., Dimitrov, M. & Minchev, C. (2004). *React. Kinet. Catal. Lett.* **83**, 299–305.